Petrogenetic significance of orthopyroxene-free garnet + clinopyroxene + plagioclase ± quartz-bearing metabasites with respect to the amphibolite and granulite facies

D. R. M. PATTISON
Department of Geology & Geophysics, University of Calgary, Calgary, AB, T2N 1 N4, Canada (pattison@geo.ucalgary.ca)

ABSTRACT
Orthopyroxene-free garnet + clinopyroxene + plagioclase ± quartz-bearing mineral assemblages represent the paragenetic link between plagioclase-free eclogite facies metabasites and orthopyroxene-bearing granulite facies metabasites. Although these assemblages are most commonly developed under $P–T$ conditions consistent with high pressure granulite facies, they sometimes occur at lower grade in the amphibolite facies. Thus, these assemblages are characteristic but not definitive of high pressure granulite facies. Compositional factors favouring their development at amphibolite grade include Fe-rich mineral compositions, Ca-rich garnet and plagioclase, and Ti-poor hornblende. The generalized reaction that accounts for the prograde development of garnet + clinopyroxene + plagioclase ± quartz from a hornblende + plagioclase + quartz-bearing (amphibolite) precursor is Hbl + Pl + Qtz = Grt + Cpx + liquid or vapour, depending on whether the reaction occurs above or below the solidus. There are significant discrepancies between experimental and natural constraints on the $P–T$ conditions of orthopyroxene-free garnet + clinopyroxene + plagioclase ± quartz-bearing mineral assemblages and therefore on the $P–T$ position of this reaction. Semi-quantitative thermodynamic modelling of this reaction is hampered by the lack of a melt model and gives results that are only moderately successful in rationalizing the natural and experimental data.

Key words: amphibolite; clinopyroxene; garnet; high pressure granulite; metabasite; orthopyroxene.

INTRODUCTION

The presence of coexisting orthopyroxene + clinopyroxene + plagioclase in metabasic bulk compositions is definitive of the granulite facies (International Union of Geological Sciences – Subcommission of the Systematics of Metamorphic Rocks; Smulikowski *et al.*, 1997). However, this association is only stable at low-intermediate pressure (domains A & B of Fig. 1). Domain A is represented by garnet-free Opx + Cpx + Pl assemblages (abbreviations of Kretz, 1983). As pressure increases, orthopyroxene reacts with plagioclase through a compositionally mediated pressure interval to produce garnet, giving rise to Grt + Cpx + Opx + Pl + Qtz assemblages (domain B of Fig. 1). The simplified reaction in the CFMAS system is:

$$Opx + Pl = Grt + Cpx + Qtz \qquad (1)$$

As pressure continues to increase, orthopyroxene is consumed (in rocks with more plagioclase than Opx) to give Opx-free Grt + Cpx + Pl + Qtz assemblages (light-grey shaded domain C of Fig. 1). At still higher pressures, plagioclase eventually ceases to be stable, giving rise to Grt + Cpx assemblages characteristic of the eclogite facies (domain D in Fig. 1).

Owing to the strong dependency on bulk composition of reaction 1, the $P–T$ boundaries between

domains A-D are not sharply defined (Green & Ringwood, 1967 and below). In intermediate pressure terranes, Grt-bearing Cpx + Pl + Qtz ± Opx-bearing assemblages may occur in close proximity to or interlayered with Grt-free Cpx + Opx + Pl + Qtz-bearing assemblages (e.g. Binns, 1964; de Waard, 1965b; Coolen, 1980; Raith *et al.*, 1990), whereas in high pressure terranes eclogite assemblages may occur in close proximity to or interlayered with Opx-free Grt + Cpx + Pl + Qtz assemblages (e.g. den Tex & Vogel, 1962; Indares *et al.*, 2003). Nevertheless, predominance of a particular mineral association in a given terrane provides a useful first-order indication of relative pressure.

Opx-free Grt + Cpx + Pl ± Qtz-bearing assemblages do not fit in either the granulite or eclogite facies as conventionally defined because they lack Opx yet contain plagioclase. Nevertheless, as shown in Fig. 1, they represent an essential paragenetic link between the two facies. Turner (1948) considered these assemblages (with hornblende) to be diagnostic of the almandine-diopside-hornblende subfacies of the granulite facies, but he later rejected this and other granulite subfacies in his later textbooks (e.g. Turner, 1968, 1981, p. 390). De Waard (1965a, 1965b, 1967) re-asserted the importance of this association as a high pressure granulite subfacies, which he termed the clinopyroxene-almandine (± hornblende) subfacies, based on natural
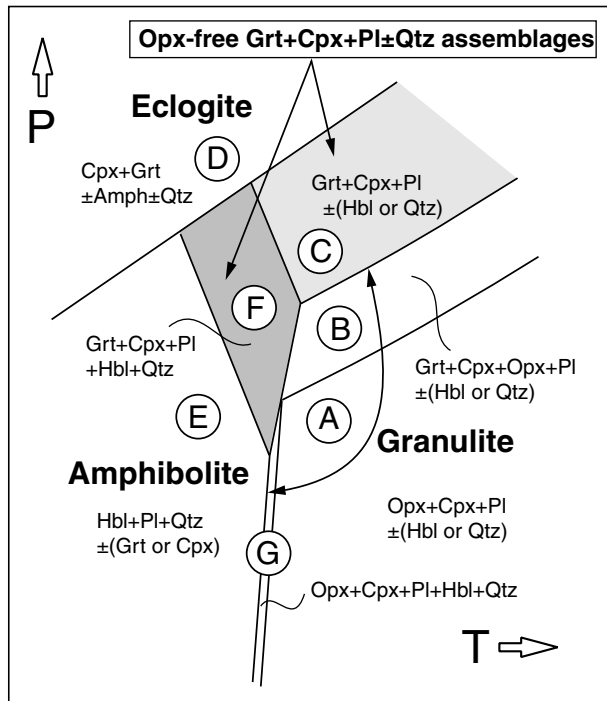
Fig. 1. Schematic *P–T* diagram showing how the *P–T* domain of Opx-free Grt + Cpx + Pl ± Qtz-bearing mineral assemblages (shaded) fits between the *P–T* domains of the commonly accepted metamorphic facies. A relatively Si-rich metabasic bulk composition is implied. The mineral assemblages listed in each field are the key subassemblages and may be accompanied by other phases depending on the bulk composition. The lettered domains are discussed in the Introduction.

assemblages and textures in the Adirondacks and elsewhere. Green & Ringwood (1967) provided experimental support for de Waard's position with their 'high pressure granulite' domain, characterized by the association Grt + Cpx + Qtz with either of Opx or plagioclase.

Although the Opx-free Grt + Cpx + Pl + Qtz association is clearly characteristic of high pressure granulite, a more controversial issue is whether it should be regarded as definitive of high pressure granulite in the way that Opx + Cpx + Pl is definitive of granulite at lower pressure. A perusal of the literature and of popular metamorphic petrology textbooks shows division on this point: some consider Grt + Cpx + Pl + Qtz to be diagnostic of high pressure granulite facies (Winkler, 1976; p. 256; Yardley, 1989; p.95; Harley, 1992; p. 325; Carswell & O'Brien, 1993), whereas others consider that it can occur in both the amphibolite and granulite facies (Bucher & Frey, 1994; p. 279; Blatt & Tracy, 1996; p. 430). The issue centres on the nature of the transition between amphibolite (domain E of Fig. 1), characterized by Hbl + Pl + Qtz assemblages with or without either Grt or Cpx, and the *P–T* domain of Opx-free   Grt + Cpx + Pl ± Hbl ± Qtz-bearing

assemblages (domain C). The transition zone is labelled F in Fig. 1 and is shaded medium-grey. The analogous transition zone between amphibolite (domain E) and intermediate pressure Opx + Cpx + Pl-bearing granulite (domain A) is the conventional amphibolite-granulite transition (domain G in Fig. 1).

It could be argued that this question is merely one of terminology and that what really matters is the *P–T* conditions at which the mineral assemblages formed. Although perhaps true in the ideal world, in reality this view seems overly optimistic. There is a large range and to some degree subjectivity in estimated *P–T* conditions of high grade rocks in the literature, a situation that can be ascribed to (1) changes over about 30 years in methods of absolute thermobarometry and (2) uncertainty over whether equilibrated mineral compositions are preserved from peak conditions. The latter question is especially problematic in high grade rocks in which non-simultaneous closure of elements as the rocks cool is to be expected (Frost & Chacko, 1989; Spear & Florence, 1992; Pattison & Bégin, 1994; Fitzsimons & Harley, 1994; Pattison *et al.*, 2003).

The value of Opx + Cpx + Pl-bearing assemblages is that not only do they define the granulite facies in metabasic bulk compositions, but they indicate a minimum temperature of formation of about 800–850 °C (in the absence of fluid infiltration) based on a large body of experimental evidence (see below). The purpose of this paper is to therefore explore whether their high pressure equivalents, namely Opx-free Grt + Cpx + Pl ± Qtz-bearing assemblages, are as definitive of granulite facies and provide as useful lower limits on temperature.

PHASE EQUILIBRIA

Figure 2 shows simplified phase equilibria for metabasites at amphibolite and granulite grade and provides a rationale for the mineral assemblage domains of Fig. 1. The most common mineral assemblage in upper amphibolite grade metabasites is Hbl + Pl ± Qtz, with or without either Cpx or garnet, so reactions involving the replacement of Hbl + Pl ± Qtz by combinations of Opx, Cpx and Grt lie at the heart of this study. Rarer Al- and Ca-poor compositions that may develop Opx at the expense of Fe-Mg orthoamphiboles (Robinson *et al.*, 1982; Schumacher *et al.*, 1990) are not considered.

Even though quartz is commonly absent from high grade metabasites, it has been included in Fig. 2 because reactions involving Hbl ± Pl with quartz occur at lower temperature than those without quartz (e.g. Binns, 1969; Spear, 1981; Rushmer, 1991; Hartel & Pattison, 1996), and our interest is in the minimum temperatures at which the Opx-free Grt + Cpx + Pl association develops (see below for further discussion of the status of quartz). In the hornblende breakdown reactions, either a hydrous volatile phase (V) or silicate melt phase (L) is generated, depending on whether the *P–T* conditions are above or below the wet solidus. The *P–T* slopes of the reactions in Fig. 1 are schematic but consistent with what is known from experiments and thermodynamic modelling (see below).

Figure 2(a) shows the arrangement of model univariant reactions around the one invariant point in the model CMASH or CFASH systems (CaO-MgO or FeO-Al$_2$O$_3$-SiO$_2$-H$_2$O). Schematic ACF diagrams (plotting method of Spear, 1993; p. 394) have been placed in the relevant divariant fields. The plotting position of the minerals is based on typical natural mineral compositions
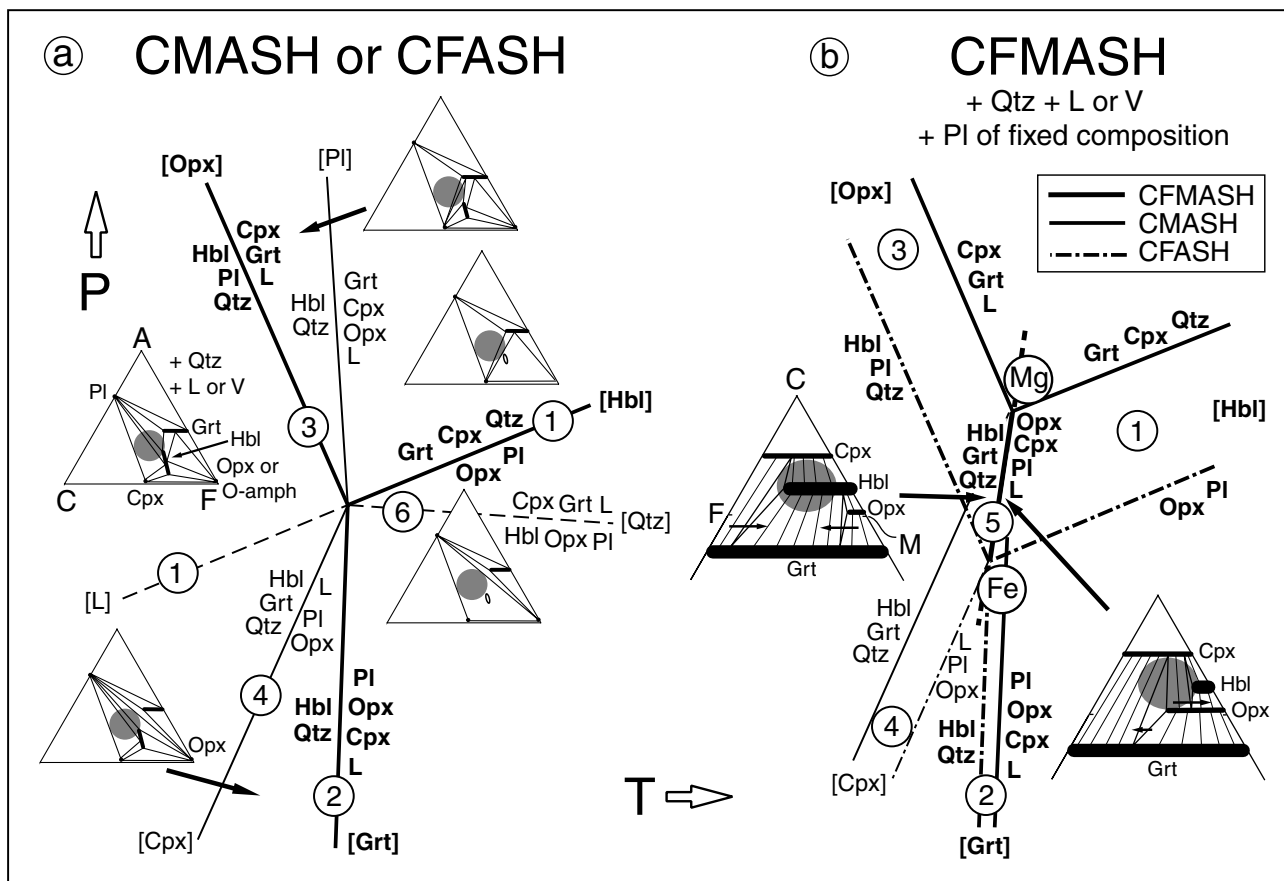
Fig. 2. Schematic *P–T* diagram showing the key phase relations involving Hbl, Pl, Qtz, Grt, Opx, Cpx and V (vapour) or L (liquid) in (a) the CFASH or CFASH systems and (b) the CFMASH system. In (a), schematic molecular ACF-type diagrams (A = Al; C = Ca; F = Fe + Mg) are inserted in each divariant field. The mineral plotting positions are based on natural mineral compositions (see text). The shaded circle represents the majority of metabasic bulk compositions (Le Maitre, 1976). Because all assemblages represented in the ACF diagram coexist with Qtz and L or V, there is no change in the topology of the diagram when either the Qtz-absent or (L or V)-absent reactions is crossed. In (b), the diagram is simplified by assuming that Qtz, Pl of fixed composition, and L or V are present in excess. The CMASH univariant curves from (a) become divariant bands in CFMASH linked by univariant curve 5. Schematic molecular 'CFM' diagrams projected from plagioclase (C = Ca – 0.5 Al; F = Fe; M = Mg) are placed immediately up-temperature and down-temperature of reaction 5. The arrows in the CFM diagrams show the migration of the three-phase triangles with increasing temperature. The shaded ellipse is the range of common metabasic bulk compositions.

(data of Hartel & Pattison, 1996), resulting in reactions relevant to modal changes observed in nature. The range of most common basaltic bulk compositions (Le Maitre, 1976) is shaded in grey.

Figure 2(b) shows the system expanded to CFMASH, in which the univariant curves from Fig. 2(a) become Fe-Mg divariant bands and the invariant point in Fig. 2(a) becomes a CFMASH univariant reaction (compare with Fig. 1). Two schematic CFM diagrams, projected from quartz and plagioclase, of fixed composition and liquid or vapour, show qualitatively the phase equilibria at higher and lower temperature than the univariant reaction. The order of Mg/(Mg + Fe) of the phases is Grt < < Opx < Hbl < Cpx, with Hbl plotting to Mg-rich side of the Cpx-Opx tie line, consistent with a trend of Mg-enrichment with rising temperature in the assemblage Hbl + Cpx + Opx (e.g. figure 19.5 of Schumacher *et al.*, 1990 and below). Arrows in the CFM diagrams show the sense of movement of the three phase triangles as temperature increases.

The idealized reactions in Fig. 2 are simplifications of natural metabasic reactions because the wide compositional ranges of natural hornblende and plagioclase result in complexities that can not be shown in the compatibility diagrams (Robinson *et al.*, 1982; Spear, 1993). In addition, the natural reactions usually involve a silicate melt phase whose composition varies with *P*, *T* and bulk composition. Multivariancy beyond that portrayed in Fig. 2(b) is introduced when Na, K, Fe^{3+}, Mn and Ti are introduced to the system, especially Na which allows a range of plagioclase compositions and Ti which may have a significant stabilizing influence on hornblende (see below). Nevertheless, the reactions in Fig. 2 are satisfactory in explaining the major changes in modal mineralogy as a function of grade and therefore represent the essentials of the natural phase equilibria (see also de Waard, 1967).
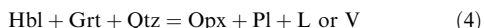
Reactions

Referring to Fig. 2, reaction 1 involves only anhydrous phases and shows how Opx-free Grt + Cpx + Pl + Qtz assemblages are the high pressure equivalent of Opx + Cpx + Pl-bearing assemblages. Reaction 2:

$$Hbl + Qtz = Opx + Cpx + Pl + L \text{ or } V \qquad (2)$$
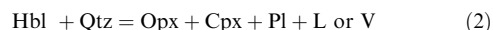
introduces the Opx + Cpx association to low-intermediate pressure metabasites and represents the classic prograde amphibolite-granulite transition reaction (domain G of Fig. 1). Reaction 3:

$$Hbl + Pl + Qtz = Grt + Cpx + L \text{ or } V \quad (3)$$

is the high pressure equivalent to reaction 2 (domain F of Fig. 1), introducing the Opx-free Grt + Cpx–bearing association of special interest to this study. Reaction 4:

$$Hbl + Grt + Qtz = Opx + Pl + L \text{ or } V \quad (4)$$

introduces a Grt + Opx association without Cpx to Ca-poor metabasites at pressures below those of reaction 1 (de Waard, 1965a & 1967 provided evidence for progress of this reaction in the Adirondacks). Reaction 5:

$$Hbl + Grt + Qtz = Opx + Cpx + Pl + L \text{ or } V \quad (5)$$
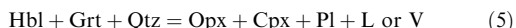
is the model CFMASH univariant reaction that links the above Fe-Mg divariant reactions.

Reactions 2 and 5 provide the low temperature limit of the diagnostic granulite association Opx + Cpx + Pl. Cursory examination of Fig. 1 shows that reaction 3 emanates to lower temperature than reactions 2 or 5.

The status of quartz in Opx-free Grt + Cpx + Pl-bearing assemblages

Whereas Grt + Cpx + Pl + Qtz-bearing assemblages, in which Qtz was present at peak conditions, necessarily indicate relatively high pressure conditions (i.e. up-pressure of reaction 1 in Fig. 2), Qtz-absent Grt + Cpx + Pl-bearing assemblages are less definitive with respect to pressure. Without quartz, reaction 1 cannot proceed in a down-pressure sense, so that these assemblages can be stable below reaction 1 in the stability field of intermediate pressure Opx + Cpx + Pl granulites. If liquid is present in abundance in the rock, the low pressure stability limit for Qtz-free Grt + Cpx ± Pl assemblages then becomes the quartz-absent reaction in Fig. 2(a):

$$Grt + Cpx + L = Hbl + Opx + Pl \quad (6)$$
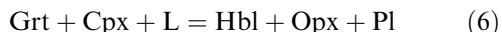
In the more likely situation in which liquid is not abundant in the rock due to mechanical considerations, the ultimate limiting reaction for Grt + Cpx stability is the anhydrous quartz-absent, olivine-producing reaction:

$$Grt + Cpx = Opx + Ol + Pl \quad (7)$$
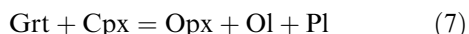
Reaction 7 is sometimes considered to be the transition reaction separating low and intermediate pressure granulite (e.g. Green & Ringwood, 1967), analogous to reaction 1 being the transition reaction between intermediate and high pressure granulite.

In mafic granulites that form from Qtz-bearing Hbl + Pl amphibolites via quartz-consuming hornblende breakdown reactions (e.g. reactions 2 & 3), quartz is usually the first mineral to be consumed because it is commonly in lower modal abundance than hornblende or plagioclase (de Waard, 1967; Hartel & Pattison, 1996). With respect to reaction 3, the result could be Qtz-free Grt + Cpx + Pl ± Hbl assemblages which are nevertheless close to being silica-saturated. Thus, even though Qtz-absent Grt + Cpx + Pl ± Hbl assemblages are permissibly stable at intermediate as well as high pressures, in practice they commonly do represent a high pressure granulite association (see below). Ways to test this possibility could include some or all of bulk compositional analysis, comparison with assemblages in interlayered rocks, analysis of reaction textures, and geobarometry.

A further complication is that even if quartz is physically present in the rock, it may not have been present as a solid phase at peak conditions. For example, Hartel & Pattison (1996) argued from textural and compositional analysis that quartz in Opx-free Grt + Cpx + Pl + Hbl rocks from the Kapuskasing Structural Zone formed from crystallization of a melt phase, now represented in the rocks by intimately distributed trondhjemitic leucosome. Thus, applying the criterion of quartz presence or absence with respect to Fig. 2 requires considerable care.

EXPERIMENTAL CONSTRAINTS

Figure 3 summarizes the many experimental constraints on reaction 2 and the relatively few experimental constraints on reaction 3, in addition to the location of the wet solidus for quartz-bearing metabasites. The data plotted in Fig. 3 pertain to the lowest grade development of the Opx + Cpx + Pl and Grt + Cpx + Pl associations. Table 1 lists some key mineral compositional parameters in the experiments to allow assessment of possible compositional control on the positions of the reactions.

To keep Fig. 3 legible, the experimental data have been omitted and lines have been drawn by eye approximately through the midpoints of the limiting experiments of the respective studies. At a given pressure, the typical temperature interval between limiting experiments is 25–50 °C, so that the lines should be considered as bands of width ± 25 °C or so. An exception is the study of Winther & Newton (1991), in which the bracket widths are 100 °C, giving rise to a ± 50 °C band. The region of overlap between reactions 2 and 3 at c. 10 kbar represents approximately where the invariant point in Fig. 1(a) occurs for the compositions of the experiments. Reaction 1, which emanates to higher temperature from this region, has been dotted in schematically as a band with a slope consistent with experimental constraints (e.g. Green & Ringwood, 1967) and thermodynamic modelling (see below).

There is considerable agreement between the various experimental studies on the slope and position of reaction 2 even though the experiments cover a fairly wide range of compositions (Table 1). Above the solidus, where it is a liquid-producing dehydration melting reaction, reaction 2 occurs in the interval 825–890 °C between 3 and 10 kbar. Below the solidus,
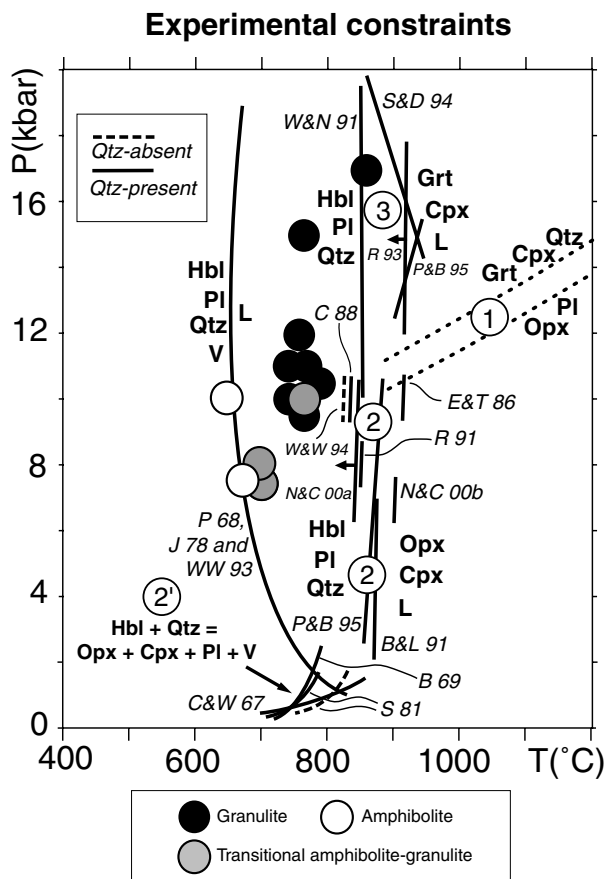
Experimental constraints

Fig. 3. Experimental data on the inception of reactions 2 and 3, and on the quartz-saturated metabasite solidus. The curves go approximately through the mid-points of the experimental brackets of the different studies (see text for further explanation). J 78 – $Pl(An_{30})$ + Qtz + H_2O solidus of Johannes (1978). P 68– wet tonalite solidus of Piwinskii (1968). WW 93– Wolf & Wyllie (1993). The three curves are so close that they have not been distinguished. All other abbreviations are listed in Table 1. The arrow on the down-temperature side of the N & C 00a curve indicates that Opx could be stable at lower temperature than the line shown, whereas the arrow on the down-temperature side of the R 93 curve indicates that Grt + Cpx could be stable at lower temperature than the line shown. The position of reaction 1 (dashed) has been inserted approximately in the P–T region separating garnet-bearing from garnet-free assemblages to facilitate comparison with Figs 1 and 2. P–T estimates for natural granulite, transitional amphibolite-granulite and amphibolite occurrences come from Table 2 and are discussed in the text.

where it is a vapour-producing dehydration reaction (reaction 2′ in Fig. 3), there is a similar spread of temperature (*c*. 75 °C). The dehydration and dehydration melting parts of reaction 2 intersect on the solidus at 2–3 kbar, 800–850 °C.

In contrast, the constraints on reaction 3 are fewer and show less agreement, although all the experiments indicate that reaction 3 occurs well above the solidus and thus will generate a melt phase rather than a hydrous vapour phase. Taking the experiments at face value, Grt + Cpx + Pl appears to develop from

Hbl + Pl + Qtz at higher pressure but at similar temperatures to Opx + Cpx.

NATURAL CONSTRAINTS

Given the limited experimental data, well documented natural settings with abundant Opx-free Grt + Cpx + Pl ± Hbl ± Qtz assemblages have been examined (Table 2). Not included in Table 2 are granulite settings which contain abundant Opx-bearing Grt + Cpx + Pl ± Hbl ± Qtz assemblages and/or show coronal reaction relationships involving these minerals. Key localities to this study are those that preserve evidence for the prograde transition from amphibolite grade assemblages to Opx-free Grt + Cpx + Pl ± Hbl ± Qtz-bearing assemblages (e.g. Kapuskasing, Furua, Mica Creek).

The localities in Table 2 are grouped according to metamorphic facies using three main criteria (details below): (1) mineral assemblages in associated rocks; (2) presence or absence of migmatization (inferred to be due to partial melting); and (3) Ti content of hornblende. Selected mineral and bulk compositional parameters are provided in Table 2 where available. To facilitate comparison, Fe in the molar Mg/(Mg + Fe) ratios in Table 2 represents total Fe as Fe^{2+} because several analyses did not distinguish between Fe^{2+} and Fe^{3+}. Bulk rock Fe^{2+}/$(Fe^{2+} + Fe^{3+})$ is typically in the range 0.7–0.9, with the exception of the severely altered Samail rocks in which $Fe^{2+}/(Fe^{2+} + Fe^{3+}) = c$. 0.2.

The P–T estimates in Table 2 come from the listed references and were generated using numerous different methods over 20 years, compromising detailed comparison between individual localities. Nevertheless, the amphibolite grade occurrences generally occur at lower temperatures than the transitional amphibolite-granulite occurrences, which in turn generally occur at lower temperatures than the granulite grade occurrences. The P–T estimates have been plotted with respect to the experimental data in Fig. 3. With one exception, all plot well below the experimentally determined position of reaction 3.

Granulite facies occurrences

Most of the localities in Table 2 are from the granulite facies, based on the occurrence of orthopyroxene in interlayered rocks or in the rocks that host the Opx-free Grt + Cpx + Pl ± Hbl ± Qtz assemblages (e.g. Fiordland). Many, although not all, show migmatitic features and contain hornblende with elevated TiO_2 contents (generally > 1.5 wt%). Other granulite localities, not listed in Table 2, which contain abundant Opx-free Grt + Cpx + Pl ± Hbl ± Qtz assemblages include the Bergen area, Norway (Griffin, 1972; Austrheim, 1987), the western parts of the Adirondack highlands (Buddington, 1939, 1963; de Waard, 1965a, 1967), parts of the Parry Sound and

Table 1. Compositions of starting minerals in experiments shown in Fig. 3.

Abbreviation in Fig. 3	Reference	Plagioclase 100 X_{An}	Hornblende or Bulk rock* 100 Mg/(Mg + Fe)	Hornblende wt% TiO$_2$
Reaction 2	**Hbl + Pl + Qtz = Opx + Cpx + L or V**			
C & W 67	Choudhuri & Winkler (1967)	n/a	86*	n/a
B 69	Binns (1969)	68–70	41–47*	n/a
S 81	Spear (1981)	42–58	60–65	0.5–1.5
E & T 86	Ellis & Thompson (1986)	100	100	0.0
C 88	Conrad et al. (1988)	44	56	1.8
R 91	Rushmer (1991)	40–45	68	1.4
B & L 91	Beard & Lofgren (1991)	48–67	58–72	0.5–1.5
W & W 94	Wolf & Wyllie (1994)	92	69	0.4
P & B 95	Patino-Douce & Beard (1995)	38	60	1.9
N & C 00a	Nair & Chacko, 2000	45	57	2.2
N & C 00b	Nair & Chacko, 2000	38	48	1.8
Reaction 3	**Hbl + Pl + Qtz = Grt + Cpx + L**			
W & N 91	Winther & Newton (1991)	n/a	48	2.0
R 93	Rushmer (1993)	55–22	68?	> 1.4
S & D 94	Sen & Dunn (1994)	51	55	1.5
P & B 95	Patino-Douce & Beard (1995)	38	60	1.9

Table 2. Selected mineral and bulk compositional parameters of natural Opx-free Grt + Cpx + Pl ± Hbl ± Qtz-bearing metabasites.

Locality	P (kbar)	T (°C)	Pl 100 X_{An}	Hbl 100 Mg/ (Mg + Fe)*	Hbl wt% TiO$_2$	Grt 100 Mg/ (Mg + Fe)*	Grt X_{Gr}^	Whole rock 100 Mg/ (Mg + Fe)*	Whole rock wt% CaO	Whole rock wt% Al$_2$O$_3$	Whole rock wt% TiO$_2$
Transitional granulite-eclogite											
Manicouagan, Quebec	16–18	850–900	32–34	n/a	n/a	42–43	25–28	51	12.7	17.4	1.1
Granulite											
Fiordland, New Zealand	13–16	> 750	28–32	58	2.1	35–42	16–30	42–56	7.2–9.9	17.6–20.0	0.9–1.5
Furua Complex, Tanzania – Zone B	9–12	750–850	27–42	42–52	1.3–2.7	28–39	17–20	40–56	6.0–10.6	13.9–18.1	1.1–2.6
Nilgiri Hills, S. India	9–10	750–800	32–49	44–63	0.8–2.0	24–38	17–22	n/a	n/a	n/a	n/a
Torngat Orogen, Labrador	10–12	750	30–40	46–53	0.8–2.1	17–32	19–28	n/a	n/a	n/a	n/a
Zambesi Belt, Zimbabwe	10–14	725–800	20–35	44–56	0.8–1.5	13–26	22–32	n/a	n/a	n/a	n/a
Kapuskasing Structural Zone, Ontario	9–11	750–800	38–47	43–55	1.2–2.0	17–21	25–28	38–48	10.0–15.4	13.4–17.2	0.8–1.8
Transitional amphibolite-granulite											
Furua Complex, Tanzania – Zone A	6–8	660–740	22–43	46–57	0.8–2.0	20–37	16–27	44–56	6.3–13.1	13.8–19.2	0.8–2.3
Chipman dyke swarm, Saskatchewan	10	750–800	40	42	1.5	11–12	28	37–45	8.9–11.4	13.0–16.9	0.6–1.8
Samail ophiolite, Oman	2–6	750–850	altered	55–65	1.0–2.0	27–37	19–30	53–62**	14.9–15.1	13.6–14.3	1.3–1.7
Gallatin Range, Montana	8	700	36–48	48–61	1.4–1.5	22–27	16–31	n/a	n/a	n/a	n/a
Amphibolite											
Mica Creek, British Columbia	7–8	650–700	32–43	39–45	0.4–0.9	11–15	29–39	36–48	8.6–11.3	13.2–16.2	1.5–2.6
Pelona Schist, California	10	650	12–16	52	0.6	10	38–42	n/a	n/a	n/a	n/a
Xenoliths											
Mojave, USA	10–12	750–800	29–46	53–72	1.0–2.6	28–42	16–22	52–62	8.7–12.0	12.5–15.9	0.8–2.5

* Molar Fe and Mg, with Fe = Fe total. ^ X_{Gr} = Ca/(Ca + Fe + Mn + Mg). ** Fe^{2+}/(Fe^{2+} + Fe^{3+}) = 0.17–0.25 in these highly altered rocks.
References: Manicouagan – Indares et al., 2000; 2003. Fiordland – Bradshaw, 1989a, 1989b, Clarke et al., 2000. Daczko et al., 2001, Furua – Coolen, 1980. Nilgiri – Raith et al., 1990. Torngat – Mengel & Rivers, 1997. Zambesi – Treloar et al., 1990. Kapuskasing – Percival, 1983, 1986; Mader et al., 1994; Hartel & Pattison, 1996. Chipman – Williams et al., 1995. Samail – Ghent & Stout, 1981. Gallatin Range – Mogk, 1992. Mica Creek – Ghent et al., 1983; Ghent & Stout, 1986; Sevigny, 1988. Pelona – Graham & Powell, 1984. Mojave – Hanchar et al., 1994.

Britt domains of the Grenville Province in Ontario (Anovitz & Essene, 1990; Tuccillo et al., 1992), and localities in Spain (den Tex & Vogel, 1962) and Ghana (von Knorring & Kennedy, 1958). The rocks from Spain and from Manicouagan (Indares et al., 2000, 2003) are interlayered with eclogite-like Pl-free Grt + Cpx-bearing rocks, indicating conditions in the transition zone between granulite and eclogite facies.

Taking the mean pressures from Table 2, the granulite occurrences span a range of 10–15 kbar, generally consistent with the experimental data in Fig. 3 and Table 1 indicating that pressures in excess of about 10 kbar are required for garnet to develop in silica-saturated metabasic compositions of intermediate Fe-Mg composition. Temperatures are generally in the range 750–800 °C.

Most of the granulite terranes in Table 2 are discrete blocks or belts of high grade rocks showing little obvious variation in grade. Two important terranes that show a transition from amphibolite rocks into Opx-free Grt + Cpx + Pl ± Hbl ± Qtz rocks are the Kapuskasing Structural Zone (Percival, 1983; Percival & West, 1994) and the Furua complex (Coolen, 1980).

Kapuskasing Structural Zone

In the Kapuskasing Structural Zone, there is a regional-scale east-ward prograde transition from Hbl + Pl ± Cpx ± Qtz-bearing amphibolites to Grt + Cpx + Pl ± Hbl ± Qtz-bearing migmatitic mafic gneisses, separated by an approximate Grt + Cpx isograd (Percival, 1983). Within the Grt + Cpx zone, gabbroic and dioritic gneisses containing Opx + Cpx + Grt + Hbl + Pl ± Qtz and paragneisses containing Opx + Grt + Pl + Bt + Qtz ± Cpx ± Sil are locally interlayered with the abundant Opx-free Grt + Cpx + Pl ± Qtz-bearing mafic gneisses, indicating that the rocks are of granulite grade. Locally, garnet in the Grt + Cpx + Pl + Hbl ± Qtz-bearing mafic gneisses is partially replaced by symplectite of Opx + Pl.

Abundant leucosome in the migmatitic mafic gneisses is Pl + Qtz-rich and is thought to represent frozen trondhjemitic liquid (Percival, 1983; Hartel & Pattison, 1996). A range of textural features combined with mass balance analysis (Hartel & Pattison, 1996) indicated the following hornblende-consuming dehydration melting reaction:

$$Hbl + Pl + Qtz = Grt + Cpx + Ttn$$
$$+ \text{trondhjemitic liquid} \qquad (6)$$
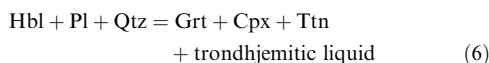
Reaction 6 is equivalent to reaction 3 in a larger chemical system. Varying progress of reaction 6 is manifested by widely varying proportions of Hbl:(Grt + Cpx) in the gneisses and is thought to have been controlled by the abundance of quartz in the protolith (Hartel & Pattison, 1996). Hartel & Pattison argued that the quartz presently in these rocks crystallized from a trondhjemitic melt phase during post-peak cooling and was not present as a solid phase at peak conditions.

Mineral compositions of the Kapuskasing rocks (Table 2) are not very different from those of the experiments on reaction 3 (Table 1), ostensibly indicating temperatures of at least 850 °C and pressures of at least 10 kbar. These elevated temperatures are consistent with the occurrence of Opx ± Grt in interlayered Bt + Pl + Qtz-bearing paragneiss, the latter indicating at least 850 °C for pressures above about 7 kbar based on numerous experimental studies (e.g. Vielzeuf & Montel, 1994; Patino Douce & Beard, 1995; Nair & Chacko, 2002; see summary in Pattison et al., 2003).

The P–T estimates from Grt-Cpx Fe-Mg exchange thermometry and multiequilibrium thermobarometry are somewhat lower, averaging 9–11 kbar, 700–800 °C (Percival, 1983; Mäder et al., 1994; Hartel & Pattison, 1996). The lower end of this range is barely above the solidus (Fig. 3), most likely indicating down-temperature Fe-Mg resetting during the slow cooling (Percival & Peterman, 1994) of the Kapuskasing rocks. Thermobarometric evidence in support of the higher temperatures comes from the locally developed Opx + Pl symplectites around garnet, which yield postpeak P–T conditions of about 7 kbar, 830 °C based on Grt-Opx Al-solubility thermobarometry corrected for late Fe-Mg exchange (Pattison et al., 2003).

Furua Complex

The Furua Complex shows the following prograde metamorphic sequence (Coolen, 1980): Zone A – amphibolite, locally containing Opx-free Grt + Cpx + Pl + Hbl ± Qtz assemblages; Zone B – domain of abundant Opx-free Grt + Cpx + Pl + Hbl ± Qtz assemblages; Zone C – granulite, containing the same assemblages as Zone B with the addition of Opx. The simplest interpretation of this sequence is that the metamorphic field gradient passed upgrade through reactions 3 (development of Grt + Cpx) and 5 (development of Opx) (see Fig. 2b).

Regarding the Zone A–Zone B transition of special interest to this study, reaction 3 seems to account well for the mineral assemblage changes. The P–T results for Zones A and B are 6–8 kbar, 660–740 °C and 8–9 kbar, 750–850 °C, respectively (Coolen, 1980), suggesting approximate conditions of 8–9 kbar, 750 °C for the Zone A–Zone B transition. Although the absolute P–T results differ modestly using more recent calibrations (e.g. Berman, 1991), Coolen's use of the same calibrations for all the zones suggests that the relative P–T differences between the zones are meaningful. The

gradient of increasing P and T between Zone A and Zone B is consistent with a number of mineral chemical contrasts between the two zones, including generally lower Ca content and higher Mg/(Mg + Fe) of garnet, higher jadeite content of Cpx, and higher Ti content of hornblende in Zone B than Zone A (Table 2 and Coolen, 1980). Few details of the outcrop features of the rocks are available to shed light on the distinction between the Opx-free Grt + Cpx + Pl + Hbl ± Qtz assemblages in Zones A and B (e.g. presence or absence of migmatization).

Regarding the Zone B–Zone C transition, P–T results augmented by trends of jadeite content in Cpx led Coolen (1980) to suggest that the Opx-bearing Cpx + Pl ± Hbl + Grt ± Qtz assemblages of Zone C formed at similar temperatures (750–850 °C) but lower pressures (7–11 kbar) than the Opx-free assemblages of Zone B. This explanation is consistent with the Zone C rocks having developed at P–T conditions within or down-pressure of reaction 1 and the Zone B rocks having developed at P–T conditions up-pressure of reaction 1 (see Fig. 2).

Transitional amphibolite-granulite facies occurrences

Transitional amphibolite-granulite occurrences are characterized by some or all of absence of orthopyroxene in any rocks, development of migmatitic features, and hornblende TiO_2 contents similar to those in the granulite grade occurrences. The Chipman dyke swarm in northern Saskatchewan (Williams et al., 1995) contains Opx-free Grt + Cpx + Pl + Hbl ± Qtz assemblages in rocks that display extensive in situ migmatitization attributed to partial melting. Although Cpx is locally present, the most conspicuous feature of these migmatized rocks is the spatial association of garnet porphyroblasts and trondhjemitic-tonalitic leucosome. The inferred dehydration melting reaction was of the form Hbl + Pl + Qtz = Grt + L, perhaps indicating slightly lower P–T conditions than for reaction 3. The P–T conditions were estimated as 10 kbar and 750–800 °C, above the wet solidus (Fig. 3) and thus consistent with the extensive migmatization observed.

The mineral compositions and P–T conditions of the Opx-free Grt + Cpx + Pl + Hbl ± Qtz assemblages in the migmatitic Gallatin gneisses (Mogk, 1990; 1992) overlap with those of Zone A of the Furua Complex (Coolen, 1980). The Opx-free Grt + Cpx + Pl + Hbl ± Qtz assemblages beneath the Samail ophiolite (Ghent & Stout, 1981) are gneissic and tectonized. Marked variations in lithology and metamorphic grade of rocks in the contact zone and local truncation of country rock layering and fabrics by the ophiolite suggest that development of the Grt-Cpx-bearing assemblages predated the tectonism associated with ophiolite emplacement, rather than having been caused by heat from the ophiolite. Pervasive alteration of the rocks, in particular plagioclase, makes pressure estimation difficult. The inferred pressure range of 2–6 kbar suggested by Ghent & Stout (1981) seems anomalously low compared to the other localities in Table 2, whereas the 750–850 °C temperature range is comparable. Overall, the mineral compositions and bulk compositions of the transitional amphibolite-granulite occurrences (Table 2) are not significantly different from those of the granulite occurrences.

Amphibolite facies occurrences

Amphibolite facies occurrences (Table 2) of Opx-free Grt + Cpx + Pl + Hbl ± Qtz assemblages are scarce compared to higher grade occurrences. They are characterized by some or all of: absence of ortho-pyroxene in any rocks; absence of migmatitic features; and relatively low Ti contents of hornblende. The best documented occurrence is at Mica Creek, British Columbia (Ghent *et al.*, 1983; Ghent & Stout, 1986). In the Pelona Schist, California, isolated occurrences of the assemblage are found in the upper part of the amphibolite zone at estimated P–T conditions of *c.* 10 kbar, 620–650 °C (Graham & Powell, 1984). The Ca and Fe content of garnet is significantly higher and the Ti content of hornblende is significantly lower in the Pelona rocks than in the higher grade occurrences listed in Table 2.

Mica Creek

In the Mica Creek area, mafic layers are found within a stratigraphic package dominated by semipelite with lesser psammite and pelite (Simony *et al.*, 1980). The mafic layers typically range in thickness between 5 cm and 5 m and are thought to represent metamorphosed basaltic sills (Sevigny, 1988). Ghent *et al.* (1983) ex-amined a Grt + Cpx isograd that separates Opx-free Grt + Cpx + Pl + Hbl ± Qtz assemblages from lower grade Hbl + Pl ± Qtz assemblages with or without Grt or Cpx. Reaction 3 seems to account well for the change in mineral assemblage across the iso-grad. With respect to isograds in interlayered metapel-itic rocks, the Grt + Cpx isograd occurs between the sillimanite-in and K-feldspar-in isograds in a sequence in which staurolite reacts out within the kyanite sta-bility field (fig. 1 of Ghent *et al.*, 1983), tightly con-straining the P–T conditions of the isograd to 7–8 kbar, 650–700 °C (Ghent *et al.*, 1983; fig. 4 of Pattison, 2001). The Grt + Cpx-bearing rocks show no evidence of migmatization in the vicinity of the isograd although interlayered metapelites are migmatized. The lack of migmatization in the metabasites suggests that if reac-tion 3 did account for the development of Grt + Cpx, it did not involve a melt phase, in contrast to the mig-matitic higher grade occurrences like Kapuskasing and Chipman. This inference fits with the P–T estimates which are slightly below the wet solidus in Fig. 3.

Compared to the granulite grade occurrences in Table 2, garnet is significantly Ca- and Fe-richer and hornblende is significantly Ti-poorer (Table 2). On the other hand, there are no obvious differences in the bulk chemistry of the rocks compared to those at granulite grade, with the possible exception of some-what lower Mg/(Mg + Fe). Approximate estimation of Fe^{3+} in Cpx from stoichiometry (Ghent *et al.*, 1983) indicates modest Fe^{3+} contents (5–12% of total Fe) that are comparable to other metabasite localities at higher grade (e.g. Pattison, 1991).

Xenoliths

Although it is not the emphasis of this study, deep crustal mafic xenoliths containing Opx-free Grt + Cpx + Pl ± Hbl ± Qtz assemblages have been widely reported in kimberlites and basaltic dykes and flows (e.g. Griffin & O'Reilly, 1987 and references therein; Hanchar *et al.*, 1994). These typically contain less hornblende than in the terrane granulites. Inferred P–T conditions and mineral compositions overlap with the terrane-scale granulite occurrences (e.g. Hanchar *et al.*, 1994; Table 2), although many extend to higher P–T conditions characteristic of the high pressure granulite-eclogite transition (Griffin & O'Reilly, 1987).

Summary of natural constraints

Opx-free Grt + Cpx + Pl ± Hbl ± Qtz assemblages occur over a wide range of grades spanning the upper amphibolite, high pressure granulite, and transitional high pressure granulite–eclogite facies, under P–T conditions ranging from 6 to 8 kbar, 650–700 °C to 14–17 kbar, 850–900 °C. These data show that (1) Opx-free Grt + Cpx + Pl-bearing assemblages are characteristic, but not definitive, of high pressure granulite facies, and (2) they are not as useful as Opx + Cpx + Pl-bearing assemblages in providing a minimum temperature of formation.
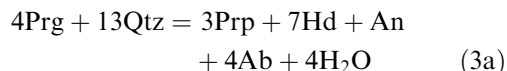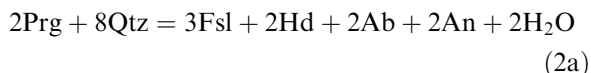
Bulk compositional factors result in a wide range of P–T conditions for the development of these assem-blages. Factors that favour their development at low (amphibolite) grade conditions include Fe-rich mineral compositions, Ca-rich garnet and Ti-poor hornblende. An additional constraint comes from the presence or absence of migmatization, assuming it can be ascribed to partial melting related to development of the assemblages: lack of migmatization suggests that the assemblage was developed by subsolidus dehydration with a_{H_2O} close to unity, whereas the presence of migmatization suggests that the assemblage was developed by super-solidus dehydration melting with a_{H_2O} less than unity. An exception would be if the assemblages developed in response to low-a_{H_2O} fluid infiltration, which might induce reaction without melting even if P–T conditions were above the H_2O-saturated solidus (see discussion below).

THERMODYNAMIC CALCULATIONS

Accepting reaction 3 as a satisfactory model for the Grt + Cpx-producing reaction, in principle it should be possible to use thermodynamic data to calculate its position and to estimate its displacement for the observed range of compositions shown in Table 2. In practice this is a particularly difficult modelling exer-cise because of the compositional and thermodynamic complexity of amphibole, the involvement of a melt phase of variable composition, and the problem of estimating water activity above the solidus.

Some semiquantitative constraints can nevertheless be provided from such calculations. Figure 4 shows diagrams calculated with the TWQ 1.02 thermodynamic data base and activity–composition expressions (Berman, 1991; Mäder *et al.*, 1994) and related phase diagram software. Similar calculations can be made using THERMOCALC software (Powell & Holland, 1988; Powell, 1998) and the thermodynamic data of Holland & Powell (1998) and Dale *et al.* (2000). Positions of invariant points for the same sets of mineral end members are in close agreement between the two data sets (Table 3). Unfortunately, neither data set has a melt model applicable to partial melting of metabasite bulk compositions.

In Fig. 4, pargasite end members of amphibole were selected for the phase diagram calculations because they provide the closest analogue to natural hornblende at amphibolite and granulite grade. In the NCMASH system, the resulting analogue reactions corresponding to 'natural' reactions 1, 2 and 3 are:

$$An + En = Di + Prp + Qtz \tag{1a}$$

$$2Prg + 8Qtz = 3Fsl + 2Hd + 2Ab + 2An + 2H_2O \tag{2a}$$

$$4Prg + 13Qtz = 3Prp + 7Hd + An + 4Ab + 4H_2O \tag{3a}$$

(abbreviations of Kretz, 1983). Although reaction 3a is a reasonable analogue to 'natural' reaction 3, significant differences include the fact that it is a dehydration rather than dehydration-melting reaction (more discussion below), and that plagioclase is product rather than a reactant. Plagioclase changes sides in the reaction because water is released as a free vapour in reaction 3a but is dissolved into the melt phase in reaction 3, and the melt phase contains a significant plagioclase component that requires plagioclase to be a reactant (e.g. see mass balance modelling of Hartel & Pattison, 1996).

Based on the data in Table 2, three sets of mineral compositions, representative of the amphibolite, granulite and high pressure granulite occurrences of the Opx-free Grt + Cpx + Pl ± Hbl ± Qtz assemblage, were created to examine how sensitive the P–T position of reaction 3 is to compositional variation. The model mineral compositions used are listed in Table 4. The granulite grade hornblende composition is based on hornblende SA1-12 from Kapuskasing (Hartel & Pattison, 1996). Variation in Ti in hornblende was accommodated assuming Ti substitution occurred by the idealized 'Ti-tschermak' exchange, $Ti^{4+} + 2Al^{3+} = (Fe,Mg)^{2+} + 2Si^{4+}$. The amphibolite, granulite and high pressure granulite end members contain 0.5, 0.2 and 0.3 cations Ti per 23-oxygen formula unit (equivalent to *c*. 0.5, 1.8 and 2.7 wt% TiO_2). The resultant hornblende compositions model the natural hornblende compositions at amphibolite grade (e.g. Ghent & Stout, 1986) satisfactorily. The 100 X_{An} in plagioclase was set at 50, 35 and 20, and 100 X_{Gr} at 40, 25 and 15, for

the amphibolite, granulite and high pressure granulite end members, respectively. Opx and Cpx were assumed to be the same composition at all grades, a reasonable first order simplification given the other uncertainties in the calculations. The observed range of bulk rock Mg/(Mg + Fe) (0.35–0.65) is shown approximately as grey bands between the Fe- and Mg-end member curves.

Figure 4(a), based on the amphibolite mineral compositions, was calculated for $a_{H_2O} = 1$ to satisfy the observations that the amphibolite grade occurrences record P–T conditions at or just below the solidus (Table 2 and Fig. 3) and show no evidence for migmatization due to partial melting. Figure 4(b–d) was calculated for the amphibolite, granulite and high pressure granulite mineral compositions, respectively, at a fixed value of a_{H_2O} of 0.3. This value of a_{H_2O} is representative of many mafic granulites (e.g. Valley *et al.*, 1990; Pattison, 1991; Mäder *et al.*, 1994) and is consistent with the common presence of migmatitic features in these rocks, indicating super-solidus conditions. Comparison of Fig. 4(a,b) shows the effect on the P–T position of the reactions due to reduction of a_{H_2O} from 1.0 to 0.3 for fixed mineral compositions, whereas comparison of Fig. 4(b-d) shows the effect of the differing mineral compositions at fixed a_{H_2O}. Also included for reference in Fig. 4 are (1) the position of the experimentally determined wet solidus for quartz-bearing metabasite from Fig. 3, and (2) the P–T estimates for the natural occurrences from Table 2.

Results

The P–T position of reaction (1a) varies markedly for the different mineral compositions, showing how the P–T boundaries between granulite, high pressure granulite and eclogite are strongly dependent on bulk composition. Reaction (3a) has a negative slope compared to the positive slope of reaction (2a) (see also Percival, 1983), consistent with the small molar volume of garnet. The inferred P–T conditions from Table 2 are consistent to a first approximation with the modelled reaction positions in that they lie within the P–T domain of Opx-free Grt + Cpx + Pl ± Hbl ± Qtz assemblages (reaction 3a), with the exception of the diagram calculated for the high pressure granulite mineral compositions (Fig. 4d) in which several of the localities plot within the P–T domain of Opx-bearing assemblages.

In detail, however, discrepancies arise. In Fig. 4(a), the reaction curves calculated at $a_{H_2O} = 1$ for the amphibolite grade mineral compositions, assuming the most common range of bulk rock Mg/(Mg + Fe) (grey band in Fig. 4a), are about 100 °C higher than the P–T conditions of the two natural settings. Reduction of a_{H_2O} from 1.0 to 0.3 (Fig. 4b) results in a down-temperature displacement of reactions (2) and (3) of 150–200 °C, allowing the grey band of normal Mg/(Mg + Fe) compositions to overlap with the amphibolite P–T conditions. Whether such a marked reduction of a_{H_2O} in

Thermodynamically predicted equilibria (TWQ 1.02)
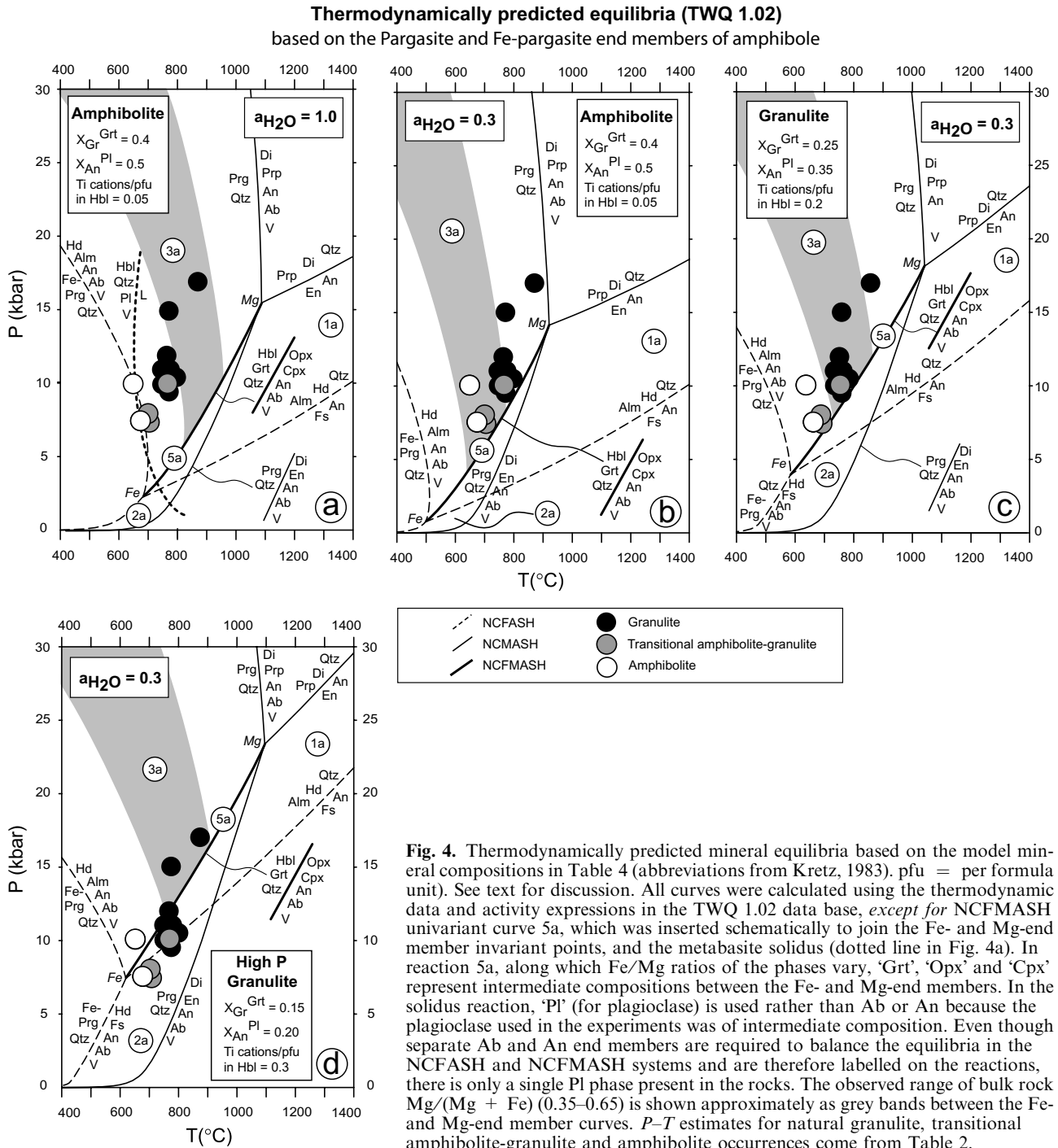based on the Pargasite and Fe-pargasite end members of amphibole

Fig. 4. Thermodynamically predicted mineral equilibria based on the model mineral compositions in Table 4 (abbreviations from Kretz, 1983). pfu = per formula unit). See text for discussion. All curves were calculated using the thermodynamic data and activity expressions in the TWQ 1.02 data base, *except for* NCFMASH univariant curve 5a, which was inserted schematically to join the Fe- and Mg-end member invariant points, and the metabasite solidus (dotted line in Fig. 4a). In reaction 5a, along which Fe/Mg ratios of the phases vary, 'Grt', 'Opx' and 'Cpx' represent intermediate compositions between the Fe- and Mg-end members. In the solidus reaction, 'Pl' (for plagioclase) is used rather than Ab or An because the plagioclase used in the experiments was of intermediate composition. Even though separate Ab and An end members are required to balance the equilibria in the NCFASH and NCFMASH systems and are therefore labelled on the reactions, there is only a single Pl phase present in the rocks. The observed range of bulk rock Mg/(Mg + Fe) (0.35–0.65) is shown approximately as grey bands between the Fe- and Mg-end member curves. *P–T* estimates for natural granulite, transitional amphibolite-granulite and amphibolite occurrences come from Table 2.

the absence of migmatization is reasonable is another question. Such a scenario would imply either that the assemblages developed due to infiltration of low-a_{H_2O} fluids (to dilute the nearly pure water produced in the dehydration reaction), or low a_{H_2O} was somehow imposed by other means. In the case of Mica Creek, there is no ready source of low a_{H_2O} fluid; even though some carbonate rock is present in the stratigraphy, the dominant lithology interlayered with the mafic rocks is

semipelite with lesser psammite and pelite (Simony *et al.*, 1980). Possible evidence for somewhat reduced a_{H_2O} in the interlayered metapelites is provided by the development of migmatite, but to what degree and over what scale this would impose reduced a_{H_2O} in the dehydrating amphibolites is uncertain.

On the other hand, the agreement between the inferred granulite *P–T* conditions and the position of reaction (3a) for the granulite mineral compositions

Table 3. Comparison of *P–T* positions of selected invariant points for pure end members using TWQ 1.02 and Holland & Powell (1998) data bases.

System	End members* at invariant pt.	TWQ 1.02		Holland & Powell (1998)	
		P (kbar)	T (°C)	P (kbar)	T (°C)
CMASH	Tr, En, Di, Prp, An, Qtz, H_2O	14.7	900	14.8	890
CFASH	Act, Fs, Hd, Alm, An, Qtz, H_2O	5.4	560	4.7	570
NCMASH	Prg, En, Di, Prp, An, Ab, Qtz, H_2O	19.1	1290	19.3	1350

*Ab – albite. Act – actinolite. Alm – almandine. An – anorthite. Di – diopside. En – enstatite. Fs – ferrosilite. Hd – hedenbergite. Prg – pargasite. Prp – pyrope. Qtz – quartz. Tr – tremolite.

Table 4. Compositions of phases used for thermodynamic modelling in Fig. 4.

Amphibolite	**(Fig. 4a,b)**
Hornblende	$[v_{0.4}Na_{0.5}K_{0.1}]$ $[Ca_{1.9}(Fe,Mg)_{0.1}]$ $(Fe,Mg)_3$ $[(Fe,Mg)_{1.35}Al_{0.6}Ti_{0.05}]$ $[Al_{1.4}Si_{2.6}]$ $Si_4[OH]_2$
Garnet	$[Ca_{0.40}(Fe,Mg)_{0.60}]_3$ $Al_2Si_3O_{12}$
Clinopyroxene	$[Ca_{0.95}(Fe,Mg)_{0.05}]$ $[(Fe,Mg)_{0.95}Al_{0.05}]$ $[Al_{0.05}Si_{1.95}]O_6$
Orthopyroxene	$(Fe,Mg)_2Si_2O_6$
Plagioclase	$[Ca_{0.5}Na_{0.5}]$ $[Al_{1.5}Si_{2.5}]O_8$
Quartz	SiO_2
a_{H_2O}	1.0 (Fig. 4a) and 0.3 (Fig. 4b)
Granulite	**(Fig. 4c)**
Hornblende	$[v_{0.4}Na_{0.4}K_{0.2}]$ $[Ca_{1.9}(Fe,Mg)_{0.1}](Fe,Mg)_3$ $[(Fe,Mg)_{1.2}Al_{0.6}Ti_{0.2}]$ $[Al_{1.7}Si_{2.3}]$ $Si_4[OH]_2$
Garnet	$[Ca_{0.25}(Fe,Mg)_{0.75}]_3$ $Al_2Si_3O_{12}$
Clinopyroxene	$[Ca_{0.95}(Fe,Mg)_{0.05}]$ $[(Fe,Mg)_{0.95}Al_{0.05}]$ $[Al_{0.05}Si_{1.95}]O_6$
Orthopyroxene	$(Fe,Mg)_2Si_2O_6$
Plagioclase	$[Ca_{0.35}Na_{0.65}]$ $[Al_{1.35}Si_{2.65}]O_8$
Quartz	SiO_2
a_{H_2O}	0.3
High *P* Granulite	**(Fig. 4d)**
Hornblende	$[v_{0.4}Na_{0.4}K_{0.2}]$ $[Ca_{1.9}(Fe,Mg)_{0.1}]$ $(Fe,Mg)_3$ $[(Fe,Mg)_{1.1}Al_{0.6}Ti_{0.3}]$ $[Al_{1.9}Si_{2.1}]$ $Si_4[OH]_2$
Garnet	$[Ca_{0.15}(Fe,Mg)_{0.85}]_3$ $Al_2Si_3O_{12}$
Clinopyroxene	$[Ca_{0.95}(Fe,Mg)_{0.05}]$ $[(Fe,Mg)_{0.95}Al_{0.05}]$ $[Al_{0.05}Si_{1.95}]O_6$
Orthopyroxene	$(Fe,Mg)_2Si_2O_6$
Plagioclase	$[Ca_{0.2}Na_{0.8}]$ $[Al_{1.2}Si_{2.8}]O_8$
Quartz	SiO_2
a_{H_2O}	0.3

(Fig. 4c), assuming the same range of Mg/(Mg + Fe) and a_{H_2O} = 0.3, is quite good. The displacement of reaction (3) going from the amphibolite to the granulite mineral compositions, at a pressure of 10 kbar and fixed a_{H_2O} = 0.3, is about 100 °C (compare Fig. 4b & c), a magnitude comparable to the difference in estimated temperature of the natural amphibolite (650–700 °C) and granulite (750–800 °C) occurrences in Table 2. This result would be more encouraging if it were not for the problem of reduced a_{H_2O} in the amphibolite occurrences. The displacement of reaction (3) going from the granulite to the high pressure granulite mineral compositions (*c*. 90 °C) results in a position of reaction (3a) that is higher than the *P–T* conditions of most of the natural settings (Fig. 4d).

DISCREPANCIES BETWEEN NATURAL, EXPERIMENTAL AND THERMODYNAMIC CONSTRAINTS ON OPX-FREE GRT + CPX + PL ± HBL ± QTZ-BEARING MINERAL ASSEMBLAGES

Comparison of the natural data in Table 2, the experimental constraints in Fig. 3 and the thermodynamic modelling in Fig. 4 reveal significant discrepancies that are difficult to resolve. A major deficiency in the thermodynamic modelling is the lack of a melt model and the consequent necessity to model the reactions using dehydration equilibria at fixed values of a_{H_2O}. The difference in slope of reactions 2 and 3 between the experiments and thermodynamic modelling (generally steeper in the experiments) may be due to the fact that the supersolidus curves in the experiments are dehydration melting reactions along which a_{H_2O} varies (decreasing from a value of 1.0 at the solidus) and which are therefore expected to have steeper slopes than the analogous dehydration curves (e.g. fig. 1 Clemens & Vielzeuf, 1987). The thermodynamically calculated displacement of reactions 2 and 3 due to varying mineral compositions (almost 200 °C between the amphibolite and high pressure granulite mineral compositions) appears to be much greater than found in the experiments. The reasons for this difference are unclear but might be due to either deficiencies in the thermodynamic modelling or a lack of compositional sensitivity in the experiments.

The *P–T* estimates for natural granulite grade Opx-free Grt + Cpx + Pl ± Hbl ± Qtz assemblages are 50–100 °C lower than implied by the dehydration melting experiments, whereas natural amphibolite occurrences of the assemblage are 150–200 °C lower. Comparison of the experimental mineral compositions in Table 1 with the natural mineral compositions in Tables 2 and 3 indicates that the experimental mineral compositions are not very different from those of the natural granulite grade minerals. Apart from possible deficiencies in our understanding of a_{H_2O} in the natural rocks, discussed above, the two main possibilities would seem to be (1) the *P–T* estimates from the natural occurrences are too low, perhaps due to late Fe-Mg resetting; (2) the relatively few vapour-absent dehydration melting experiments on reaction 3 were overstepped due to sluggish reaction kinetics in the relatively low experimental temperature range of 700–800 °C. Whereas resetting might partially account for the temperature underestimates in the granulite occurrences, the *P–T* constraints on the amphibolite occurrences (e.g. Mica Creek) are based on robust mineral assemblage constraints that are unaffected by resetting. In summary, there seems to be a need for targeted experiments and accompanying thermodynamic modelling on this problem, perhaps informed by the constraints presented in this study.

ACKNOWLEDGEMENTS

REFERENCES

Anovitz, L. M. & Essene, E. J., 1990. Thermobarometry and pressure-temperature paths in the Grenville Province of Ontario. *Journal of Petrology*, **31**, 197–241.

Austrheim, H., 1987. Eclogitization of lower crustal granulites by fluid migration through shear zones. *Earth and Planetary Science Letters*, **81**, 221–232.

Beard, J. S. & Lofgren, G. E., 1991. Dehydration melting and water-saturated melting of basaltic and andesitic greenstones and amphibolites at 1, 3, and 6.9 kbar. *Journal of Petrology*, **32**, 365–401.

Berman, R. G., 1991. Thermobarometry using multi-equilibrium calculations: a new technique, with petrological applications. *Canadian Mineralogist*, **29**, 833–855.

Binns, R. A., 1964. Zones of progressive regional metamorphism in the Willyama Complex, Broken Hill district, New South Wales. *Journal of the Geological Society of Australia*, **11**, 283–330.

Binns, R. A., 1969. Hydrothermal investigations of the amphibolite–granulite facies boundary. *Special Publication of the Geological Society of Australia*, **2**, 341–344.

Blatt, H. & Tracy, R. J., 1996. *Petrology: Igneous, Sedimentary, and Metamorphic*. New York: W.H. Freeman.

Bradshaw, J. Y., 1989a. Early Cretaceous vein-related garnet granulite in Fiorland, southwest New Zealand: a case for infiltration of mantle-derived CO_2-rich fluids. *Journal of Geology*, **97**, 697–717.

Bradshaw, J. Y., 1989b. Origin and metamorphic history of an Early Cretaceous polybaric granulite terrain, Fiordland, southwest New Zealand. *Contributions to Mineralogy and Petrology*, **103**, 346–360.

Bucher, K. & Frey, M., 1994. *Petrogenesis of Metamorphic Rocks*. Berlin: Springer-Verlag.

Buddington, A. F., 1939. Adirondack igneous rocks and their metamorphism. *Geological Society of America Memoir*, **7**, 1–354.

Buddington, A. F., 1963. Isograds and the role of H_2O in metamorphic facies of orthogneisses of the northwest Adirondack area, New York. *Geological Society of America Memoir*, **74**, 1155–1182.

Carswell, D. A. & O'Brien, P. J., 1993. Thermobarometry and geotectonic significance of high-pressure granulites: examples from the Moldanubian Zone of the Bohemian Massif in Lower Austria. *Journal of Petrology*, **34**, 427–459.

Choudhuri, A. & Winkler, H. G. F., 1967. Anthophyllit und hornblende in einigen metamorphen reaktionen. *Contributions to Mineralogy and Petrology*, **14**, 293–315.

Clarke, G. L., Klepeis, K. A. & Daczko, N. R., 2000. Cretaceous high-P granulites at Milford Sound, New Zealand: metamorphic history and emplacement in a convergent margin setting. *Journal of Metamorphic Geology*, **18**, 359–374.

Clemens, J. D. & Vielzeuf, D., 1987. Constraints on melting and magma production in the crust. *Earth and Planetary Science Letters*, **86**, 287–306.

Conrad, W. K., Nicholls, I. A. & Wall, V. J., 1988. Water-saturated and undersaturated melting of metaluminous and peraluminous crustal compositions at 10 kb: Evidence for the origin of silicic magmas in the Taupo Volcanic Zone, New Zealand, and other occurrences. *Journal of Petrology*, **29**, 765–803.

Coolen, J. J. M. M. M., 1980. Chemical Petrology of the Furua Granulite Complex, Southern Tanzania. *GUA Papers of Geology – Series*, **1**, 13–1980.

Daczko, N. R., Clarke, G. L. & Klepeis, K. A., 2001. Transformation of two-pyroxene hornblende granulite to garnet granulite involving simultaneous melting and fracturing of the lower crust, Fiordland, New Zealand. *Journal of Metamorphic Geology*, **19**, 547–560.

Dale, J., Holland, T. J. B. & Powell, R., 2000. Hornblende-garnet-plagioclase thermobarometry: a natural assemblage calibration of the thermodynamics of hornblende. *Contributions to Mineralogy and Petrology*, **140**, 353–362.

Ellis, D. J. & Thompson, A. B., 1986. Subsolidus and partial melting reactions in the quartz-excess $CaO + MgO + Al_2O_3 + SiO_2 + H_2O$ system under water-excess and water-deficient conditions to 10 kb: Some implications for the origin of peraluminous melts from mafic rocks. *Journal of Petrology*, **27**, 91–121.

Fitzsimons, I. C. W. & Harley, S. L., 1994. The influence of retrograde cation exchange on granulite *P-T* estimates and a convergence technique for the recovery of peak metamorphic conditions. *Journal of Petrology*, **35**, 543–576.

Frost, B. R. & Chacko, T., 1989. The granulite uncertainty principle: Limitations on thermobarometry in granulites. *Journal of Geology*, **97**, 435–450.

Ghent, E. D. & Stout, M. Z., 1981. Metamorphism at the base of the Samail Ophiolite, southeastern Oman mountains. *Journal of Geophysical Research, 86-*, **B4**, 2557–2571.

Ghent, E. D. & Stout, M. Z., 1986. Garnet-hornblende thermometry, $CaMgSi_2O_6$ activity, and the minimum pressure limits of metamorphism for garnet amphibolites. *Journal of Geology*, **94**, 736–743.

Ghent, E. D., Stout, M. Z. & Raeside, R. S., 1983. Plagioclase-clinopyroxene-garnet-quartz equilibria and the geobarometry and geothermometry of garnet amphibolites from Mica Creek, British Columbia. *Canadian Journal of Earth Sciences*, **20**, 699–706.

Graham, C. M. & Powell, R., 1984. A garnet-hornblende geothermometer: calibration, testing, and application to the pelona schist, southern California. *Journal of Metamorphic Geology*, **2**, 13–31.

Green, D. H. & Ringwood, A. E., 1967. An experimental investigation of the gabbro to eclogite transition and petrological implications. *Geochimica et Cosmochimica Acta*, **31**, 767–833.

Griffin, W. L., 1972. Formation of eclogites and the coronas in anorthosites, Bergen Arcs, Norway. *Geological Society of America Memoir*, **135**, 37–63.

Griffin, W. L. & O'Reilly, S. Y., 1987. The composition of the lower crust and the nature of the continental Moho – xenolith evidence. In: *Mantle Xenoliths* (Nixon, P. H., ed.). London: Wiley, 413–430.

Hanchar, J. M., Miller, C. F., Wooden, J. L., Bennett, V. C. & Staude, J. G., 1994. Evidence from xenoliths for a dynamic lower crust, eastern Mojave desert, California. *Journal of Petrology*, **35**, 1377–1415.

Harley, S. L., 1992. Proterozoic granulite terranes. In: *Proterozoic Crustal Evolution, Developments in Precambrian Geology, 10* (Condie, K. C., ed.), 301–359. Elsevier, Amsterdam.

Hartel, T. H. D. & Pattison, D. R. M., 1996. Genesis of the Kapuskasing (Ontario) migmatitic mafic granulites by dehydration melting of amphibolite: the importance of quartz to reaction progress. *Journal of Metamorphic Geology*, **14**, 591–611.

Holland, T. J. B. & Powell, R., 1998. An internally consistent thermodynamic data set for phases of petrological interest. *Journal of Metamorphic Geology*, **16**, 309–344.

Indares, A., Dunning, G. & Cox, R., 2000. Tectono-thermal evolution of deep crust in a Mesoproterozoic continental collision setting: the Manicouagan example. *Canadian Journal of Earth Sciences*, **37**, 325–340.

Indares, A. *et al.*, 2003. Metamorphic textures and *P–T* evolution of high-*P* granulites from the Helukuau Terrane, NE Grenville Province. *Journal of Metamorphic Geology*, **21**, 35–48.

von Knorring, O. & Kennedy, W. Q., 1958. The mineral paragenesis and metamorphic status of garnet-hornblende-pyroxene-scapolite gneiss from Ghana. *Mineralogical Magazine*, **31**, 546–559.

Kretz, R., 1983. Symbols for rock-forming minerals. *American Mineralogist*, **68**, 277–279.

Le Maitre, R. W., 1976. The chemical variability of some common igneous rocks. *Journal of Petrology*, **17**, 589–637.

Mäder, U.K., Percival, J. A. & Berman, R. G., 1994. Thermo-barometry of garnet-clinopyroxene-hornblende granulites from the Kapuskasing structural zone. *Canadian Journal of Earth Sciences*, **31**, 1134–1145.

Mengel, F. & Rivers, T., 1997. Metamorphism in the Paleoproterozoic Torngat orogen, Labrador: petrology and P-T-t paths of amphibolite- and granulite-facies rocks across the Komaktorvik shear zone. In: *Tectonometamorphic Studies of the Canadian Shield (Part 1)* (Berman, R. G. & Easton, R. M., eds). Canadian Mineralogist, **35**, 1137–1160.

Mogk, D. W., 1990. A model for the granulite–migmatite association in the Archean basement of southwestern Montana. In: *Granulites and Crustal Evolution* (D. Vielzeuf, Ph & Vidal, Ph, eds), 133–155. Kluwer, Dordrecht

Mogk, D. W., 1992. Ductile shearing and migmatization at mid-crustal levels in an Archean high grade gneiss belt, northern Gallatin Range, Montana, USA. *Journal of Metamoprhic Geology*, **10**, 427–438.

Nair, R. & Chacko, T., 2000. Fluid-Absent Melting of Two High Grade Amphibolites: Constraints on the Conditions Required for Orthopyroxene Formation. *Geological Association of Canada – Mineralogical Association of Canada Annual Meeting*, Abstracts with Program, 24, (on CD only).

Nair, R., & Chacko. T., 2002. Fluid-absent melting of high-grade semi-pelites: *P-T* constraints on orthopyroxene formation and implications for granulite genesis. *Journal of Petrology*, in press.

Patino Douce, A. E. & Beard, J. S. Dehydration melting of biotite gneiss and quartz amphibolite from 3 to 15 kbar. *Journal of Petrology*, **36**, 707–738.

Pattison, D. R. M., 1991. Infiltration-driven dehydration and anatexis in granulite facies meragabbro, Grenville Province, Ontario. *Canada Journal of Metamorphic Geology*, **9**, 315–332.

Pattison, D. R. M., 2001. Instability of Al_2SiO_5 'triple point' assemblages in muscovite + biotite + quartz-bearing metapelites, with implications. *American Mineralogist*, **86**, 1414–1422.

Pattison, D. R. M. & Bégin, N. J., 1994. Zonong patterns in orthopyroxene and garnet in granulites: implications for geothermometry. *Journal of Metamorphic Geology*, **12**, 387–410.

Pattison, D. R. M., Chacko, T., Farquhar, J. & McFarlane, C. R. M., 2003. Temperatures of granulite-facies metamorphism: constraints from experimental phase equilibria and thermobarometry corrected for retrograde exchange. *Journal of Petrology*, in press.

Percival, J. A., 1983. High-grade metamorphism in the Chapleau-Foleyet area, Ontario. *American Mineralogist*, **68**, 667–686.

Percival, J. A., 1986. The Kapuskasing uplift: *Archean Greenstones and Granulites. Ottawa 1986 meeting, Field trip 16 guidebook*. Geological Association of Canada, Ottawa.

Percival, J. A. & Peterman, Z. E., 1994. Rb-Sr biotite and whole rock data from the Kapuskasing uplift and their bearing on the cooling and exhumation history. *Canadian Journal of Earth Sciences*, **31**, 1172–1181.

Percival, J. A. & West, G. F., 1994. The Kapuskasing uplift: a geological and geophysical synthesis. *Canadian Journal of Earth Sciences*, **31**, 1256–1286.

Powell, R., 1998. Calculating phase diagrams involving solid solutions via non-linear equations, with examples using THERMOCALC. *Journal of Metamorphic Geology*, **16**, 577–588.

Powell, R. & Holland, T. J. B., 1988. An internally consistent thermodynamic data set with uncertainties and correlations: 3. Application methods, a worked example and a computer program. *Journal of Metamorphic Geology*, **6**, 173–204.

Raith, M., Srikantappa, C., Ashamanjari, K. G. & Spiering, B., 1990. The granulite terrane of the Nilgiri Hills (southern India): Characterization of high grade metamorphism. In: *Granulites and Crustal Evolution* (Vielzeuf, D. & Vidal, Ph, eds), 339–365. Kluwer, Dordrecht.

Robinson, P., Spear, F. S., Schumacher, J. C., Laird, J., Klein, C., Evans, B. W. & Doolan, B. L., 1982. Phase relations of metamorphic amphiboles: natural occurrence and theory. In: *Amphiboles: Petrology and Experimental Phase Relations. Reviews in Mineralogy, 9B*, (Veblen, D. R. & Ribbe, P. H., eds), 1–227. Mineralogical Society of America, Washington DC.

Rushmer, T., 1991. Partial melting of two amphibolites: contrasting experimental results under fluid-absent conditions. *Contributions to Mineralogy and Petrology*, **107**, 41–59.

Rushmer, T., 1993. Experimental high pressure granulites: Some applications to natural mafic xenolith suites and Archean granulite terranes. *Geology*, **21**, 411–414.

Schumacher, J. C., Hollocher, K. T., Robinson, P. & Tracy, R. J., 1990. Progressive reactions and melting in the Acadian metamorphic high of central Massachusetts and southwestern New Hampshire, USA. In: *High Temperature Metamorphism and Crustal Anatexis, Mineralogical Society Series, 2.* (Ashworth, J. R. & Brown, M., eds), 272–315. Unwin-Hyman, London.

Sen, C. & Dunn, T., 1994. Dehydration melting of a basaltic composition amphibolite at 1.5 and 2.0 GPa: implications for the origin of adakites. *Contributions to Mineralogy and Petrology*, **117**, 394–409.

Sevigny, J. H., 1988. Geochemistry of Late Proterozoic amphibolites and ultramafic rocks, southeastern Canadian Cordillera. *Canadian Journal of Earth Sciences*, **25**, 1323–1337.

Simony, P. S., Ghent, E. D., Craw, D., Mitchell, W. & Robbins, D. B., 1980. Structural and metamorphic evolution of northeast flank of Shuswap complex, southern Canoe River area, British Columbia. *Geological Society of America Memoir*, **153**, 445–461.

Smulikowski, W., Desmons, J., Harte, B., Sassi, F. P. & Schmid, R., 1997. Towards a unified nomenclature of metamorphism: 3 *Types, Grades and Facies*. International Union of Geological Sciences – Subcommission of the Systematics of Metamorphic Rocks (SCMR). Work in progress.

Spear, F. S., 1981. An experimental study of hornblende stability and compositional variability in amphibolite. *American Journal of Science*, **281**, 697–734.

Spear, F. S., 1993. *Metamorphic Phase Equilibria and Pressure-Temperature-Time Paths, Monograph, 1.* Mineralogical Society of America, Washington DC.

Spear, F. S. & Florence, F. P., 1992. Thermobarometry in granulites: pitfalls and new approaches. In: *The Archean Limpopo Granulite Belt: Tectonics and Deep Crustal Processes* (van Reenan, D. D., Roering, C., Ashwal, L. D. & de Wit, M. J., eds) *Precambrian Research*, **55**, 209–241.

den Tex, E. & Vogel, D. E., 1962. A 'granulitgebirge' at Cabo Ortegal, N.W. Spain. *Geological Rundschau*, **52**, 954–112.

Treloar, P. J., Carney, J. N., Crow, M. J., Evans, J. A. & Barton, C. N., 1990. Pressure-temperature-time paths of granulite metamorphism and uplift, Zambesi Belt, Zimbabwe. In: *Granulites and Crustal Evolution* (Vielzeuf, D. & Vidal, Ph, eds), 223–241. Kluwer, Dordrecht.

Tuccillo, M. E., Mezger, K., Essene, E. J. & van der Pluijm, B. A., 1992. Thermobarometry, geochronology and the interpretation of P-T-t data in the Britt domain, Ontario Grenville Orogen, Canada. *Journal of Petrology*, **33,** 1225–1259.

Turner, F. J., 1948. Mineral and structural evolution of the metamorphic rocks. *Geological Society of America Memoir*, **30,** 1–342.

Turner, F. J., 1968., 1st edn; 1981, 2nd edn. *Metamorphic Petrology*. McGraw-Hill, New York.

Valley, J. W., Bohlen, S. R., Essene, E. J. & Lamb, W., 1990. Metamorphism in the Adirondacks. II. The role of fluids. *Journal of Petrology*, **31,** 555–596.

Vielzeuf, D. & Montel, J. M., 1994. Partial melting of metagreywackes. Part I. Fluid-absent experiments and phase relationships. *Contributions to Mineralogy and Petrology*, **117,** 375–393.

de Waard, D., 1965a. The occurrence of garnet in the granulite-facies terrane of the Adirondack Highlands. *Journal of Petrology*, **6,** 165–191.

de Waard, D., 1965b. A proposed subdivision of the granulite facies. *American Journal of Science*, **263,** 455–461.

de Waard, D., 1967. The occurrence of garnet in the granulite-facies terrane of the Adirondack Highlands and elsewhere, an amplification and a reply. *Journal of Petrology*, **8,** 213–232.

Williams, M. L., Hanmer, S., Kopf, C. & Darrach, M., 1995. Syntectonic generation and segregation of tonalitic melts from amphibolite dikes in the lower crust, Striding-Athabasca mylonite zone, northern Saskatchewan. *Journal of Geophysical Research*, **100,** 15,717–15,734.

Winkler, H. G. F., 1976. *Petrogenesis of Metamorphic Rocks.* Springer-Verlag, New York.

Winther, K. T. & Newton, R. C., 1991. Experimental melting of hydrous low-K tholeiite: evidence on the origin of Archaean cratons. *Bulletin of the Geological Society of Denmark*, **39,** 213–228.

Wolf, M. B. & Wyllie, P. J., 1994. Dehydration-melting of amphibole at 10kbar: the effects of temperature and time. *Contributions to Mineralogy and Petrology*, **115,** 369–383.

Wyllie, P. J. & Wolf, M. B., 1993. Amphibolite dehydration-melting: sorting out the solidus. In: *Magmatic Processes and Plate Tectonics, Special publication, 76,* (Prichard, H. M., Alabaster, T., Harris, N. B. W. & Neary, C. R., eds), 405–416. Geological Society, London.

Yardley, B. W. D., 1989, .*An Introduction to Metamorphic Petrology*. Longman Scientific, Harlow.